doi:10.1016/S0022-2836(02)00370-4 available online at http://www.idealibrary.com on IDEAL® J. Mol. Biol. (2002) 319, 449–461

JMB

Minor Structural Changes in a Mutated Human Melanoma Antigen Correspond to Dramatically Enhanced Stimulation of a CD4+ Tumor-infiltrating Lymphocyte Line

Eric J. Sundberg[1]*, Mark W. Sawicki[2], Scott Southwood[3] Peter S. Andersen[4], Alessandro Sette[3] and Roy A. Mariuzza[1]

[1]*Center for Advanced Research in Biotechnology, W. M. Keck Laboratory for Structural Biology, University of Maryland Biotechnology Institute, 9600 Gudelsky Drive Rockville, MD 20850, USA*

[2]*BSI Proteomics Corporation Gaithersburg, MD 20877, USA*

[3]*Epimmune Corporation, San Diego, CA 92121, USA*

[4]*Symphogen A/S, Elektrovej Building 375, DK-2800 Lyngby Denmark*

**Corresponding author*

While most immunotherapies for cancer have focused on eliciting specific $CD8^+$ cytotoxic T lymphocyte killing of tumor cells, a mounting body of evidence suggests that stimulation of anti-tumor $CD4^+$ T cell help may be required for highly effective therapy. Several MHC class II-restricted tumor antigens that specifically activate such $CD4^+$ helper T lymphocytes have now been identified, including one from a melanoma tumor that is caused by a single base-pair mutation in the glycolytic enzyme triosephosphate isomerase. This mutation results in the conversion of a threonine residue to isoleucine within the antigenic epitope, concomitant with a greater than five log-fold increase in stimulation of a $CD4^+$ tumor-infiltrating lymphocyte line. Here, we present the crystal structures of HLA-DR1 in complex with both wild-type and mutant TPI peptide antigens, the first structures of tumor peptide antigen/MHC class II complexes recognized by $CD4^+$ T cells to be reported. These structures show that very minor changes in the binding surface for T cell receptor correspond to the dramatic differences in T cell stimulation. Defining the structural basis by which $CD4^+$ T cell help is invoked in an anti-tumor immune response will likely aid the design of more effective cancer immunotherapies.

Keywords: X-ray crystallography; major histocompatibility complex; T cell stimulation; melanoma; tumor antigen

Introduction

Harnessing the power and specificity of cellular immunity is becoming a viable therapeutic alternative for cancer treatment. While this implies directing $CD4^+$ and/or $CD8^+$ T cell responses towards tumor eradication, current approaches to cancer immunotherapy have focused predominantly on $CD8^+$ T cells for a number of reasons: most tumors are major histocompatibility complex (MHC) class I positive, while displaying no MHC class II molecules; $CD8^+$ cytotoxic T lymphocytes (CTLs) have the ability to lyse tumor cells directly; and, due to differences in the MHC class I and II antigen processing pathways, the identification of MHC class I-restricted tumor antigens has been relatively easier than isolation of their MHC class II-restricted counterparts. Several of these MHC class I-restricted tumor antigens have now been used clinically as cancer vaccines. Although there

Abbreviations used: $A2_{103-117}$, HLA-A2 endogenous peptide, residues 103–117; APC, antigen presenting cell; ARB, average relative binding; ASA, accessible surface area; CD40L, CD40 ligand; CDR, complimentarity determining region; CTL, cytotoxic T lymphocyte; DC, dendritic cell; $HA_{306-318}$, hemaglutinin antigenic peptide, residues 306–318; HLA, human leukocyte antigen; HTL, helper T lymphocyte; IC_{50}, 50% inhibitory concentration; MHC, major histocompatibility complex; P, position; pMHC, peptide–MHC; S_c, shape complimentarity; SEC3, staphylococcal enterotoxin C3; SEC3-3B2, staphylococcal enterotoxin C3 phage display variant 3B2; TCR, T cell receptor; TPI, triosephosphate isomerase; TPI_{23-37}, triosephosphate isomerase antigenic peptide, residues 23–37; TIL, tumor-infiltrating lymphocyte.

E-mail address of the corresponding author: sundberg@umbi.umd.edu

0022-2836/02/$ - see front matter

is evidence of positive therapeutic effects, the clinical responses of patients treated with such vaccines have been generally less than had been expected from CTL activities *in vitro*.[1–4]

These weak and transient $CD8^+$-directed immune responses when using MHC class I-restricted tumor antigens as vaccines may be due to a lack of any corroborating $CD4^+$-specific anti-tumor response. Indeed, several recent studies have implicated important roles for $CD4^+$ helper T lymphocytes (HTLs) in both the initiation and maintenance of $CD8^+$ immune responses against cancer, as well as tumor growth inhibition even in the absence of $CD8^+$ T cells.[5–8]

Optimal priming of $CD8^+$ T cell responses has been shown to require specific $CD4^+$ T cell help, even against MHC class II negative tumors.[9] $CD4^+$ HTLs and $CD8^+$ CTLs, thus, need not recognize antigens on the same antigen presenting cell (APC), as $CD4^+$ T cells can provide help through intermediary professional APCs such as dendritic cells (DCs). CD40 ligand (CD40L) expressed on the surface of $CD4^+$ HTLs interacts with CD40 on DCs, empowering them for effective priming and activation of tumor-specific $CD8^+$ CTLs.[10–14] Several distinct post-priming effects of $CD4^+$ HTLs on $CD8^+$ anti-tumor responses have been characterized, including maintenance of CTL numbers and functionality, as well as facilitation of tumor infiltration by CTLs.[15]

The growing body of evidence implicating crucial roles for $CD4^+$ T cell help in tumor eradication has coincided with viable techniques for the isolation of MHC class II-restricted tumor antigens.[16] While their identification still lags that of their MHC class I-restricted counterparts, the database of MHC class II-restricted tumor antigens now encompasses a variety of cancer types and allelic restrictions.[7,8]

One recently described MHC class II-restricted human melanoma tumor antigen derives from a mutated form of the glycolytic enzyme triosephosphate isomerase (TPI), in which a cytosine to thiamine base-pair mutation converts a single Thr residue to an Ile.[17] Presentation of wild-type and mutant TPI peptides encompassing residues 23–37 (TPI_{23-37}), and including the mutation site at residue 28, by HLA-DR1 resulted in dramatically different T cell stimulatory activities in which stimulation of the $CD4^+$ tumor-infiltrating lymphocyte (TIL) line 1558 was enhanced more than five log-fold for the mutant relative to the wild-type TPI_{23-37} peptide. T cell activation assays using a series of truncated mutant TPI_{23-37} peptides to stimulate TIL 1558 suggested that the mutation site residue lies at position P3 of the peptide, and thus likely contributes specific intermolecular contacts with the T cell receptor (TCR).

In order to better understand the structural basis for $CD4^+$ T cell responses to MHC class II-restricted tumor antigens in general and for the dramatically altered T cell stimulatory capacities of the wild-type and mutant TPI_{23-37} peptides specifically, we have determined the structures of both peptides in complex with HLA-DR1. We confirm that the mutation site residue lies at position P3 and show that extremely minor structural changes at the mutation site associated with the putative TCR interface are responsible for the differential T cell activation by the wild-type and mutant TPI_{23-37} peptides.

Results

Overview of the wild-type and mutant TPI_{23-37} peptide/HLA-DR1 structures

We have solved the crystal structures of both wild-type and mutant TPI_{23-37} peptide antigen in complex with HLA-DR1. As in the structure determination of a human collagen II peptide in complex with HLA-DR4,[18] we co-crystallized the TPI_{23-37}/HLA-DR1 complex with a superantigen to facilitate the growth of large and well diffracting crystals. In this case, we used the 3B2 variant of staphylococcal enterotoxin C3 (SEC3-3B2), which

Table 1. Data collection and refinement statistics for the wild-type and mutant TPI_{23-37} peptide/HLA-DR1/SEC3-3B2 complexes

	Wild-type	Mutant
A. *Data collection*		
Space group	*R*3	*R*3
Cell dimensions		
a (Å)	171.3	173.0
c (Å)	121.0	121.4
Temperature (K)	100	100
Resolution limit (Å)	1.93	2.40
Unique reflections	99,361	52,723
Total observations	311,680	154,803
Completeness (%)	99.8 (98.1)[a]	99.6 (99.8)
Mean $I/\sigma(I)$	13.9 (2.0)	12.1 (1.8)
R_{sym} (%)[b]	9.5 (47.9)	11.6 (59.0)
B. *Refinement*		
R_{free}[c]	22.0 (23.4)	24.5 (32.0)
R_{cryst}	20.8 (25.4)	20.5 (28.5)
Protein		
Residues	614	610
Average *B* (Å^2)	26.5	33.0
Water		
Molecules	405	275
Average *B* (Å^2)	31.7	32.8
RMS deviations from ideality		
Bonds (Å)	0.007	0.007
Angles (°)	1.519	1.378
Ramachandran plot statistics		
Core (%)	87.7	88.1
Allowed (%)	11.4	11.1
Generous (%)	0.7	0.6
Disallowed (%)	0.2	0.2

[a] Values in parentheses correspond to the highest resolution shell: wild-type (1.96–1.93 Å); mutant (2.44–2.40 Å).

[b] $R_{sym} = \sigma|I - \langle I\rangle|/\sigma\langle I\rangle$, where I is the observed intensity and $\langle I\rangle$ is the average intensity of multiple observations of symmetry-related reflections.

[c] A portion of the overall reflections was set aside for R_{free} calculations: wild-type (4240 reflections, 4.3%); mutant (2131 reflections, 4.0%).

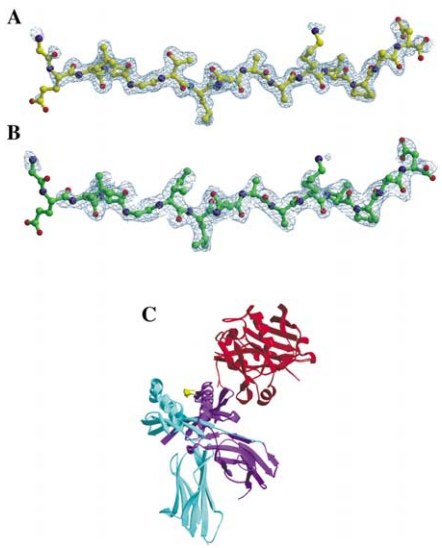

Figure 1. The wild-type and mutant TPI_{23-37} peptide/HLA-DR1/SEC3-3B2 complex structures. σ_A-Weighted $2F_o - F_c$ electron density maps in which the TPI_{23-37} peptide atoms have been omitted from the map calculation for (a) the wild-type TPI_{23-37} peptide and (b) the mutant TPI_{23-37} peptide. Maps are contoured at 1.0σ. (c) Superposition of the overall wild-type and mutant TPI_{23-37} peptide/HLA-DR1/SEC3-3B2 complex structures. In all panels, colors are as follows: wild-type TPI_{23-37} peptide, yellow; mutant TPI_{23-37} peptide, green; HLA-DR1 α chain, purple; HLA-DR1 β chain, cyan; SEC3-3B2, red; nitrogen atoms, blue; oxygen atoms and water molecules, red. (a) and (b) produced using Bobscript[61] and Raster3D.[62] (c) and subsequent Figures produced using MOLSCRIPT[63] and Raster3D,[62] unless otherwise noted.

had been produced by phage display and exhibits a 50-fold higher affinity for HLA-DR1 than does wild-type SEC3.[19] Both wild-type and mutant TPI_{23-37} peptide/HLA-DR1/SEC3-3B2 complex structures were solved individually by molecular replacement methods using HLA-DR1[20] and wild-type SEC3[21] as search models and refined independently to nominal resolutions of 1.93 and 2.40 Å, respectively. Data collection and refinement statistics are shown in Table 1 and σ_A-weighted omit electron density maps for the TPI_{23-37} peptides are shown in Figure 1(a) and (b).

The overall complex structures are shown in Figure 1(c). Importantly, SEC3-3B2 interacts only with regions of the HLA-DR1 α subunit outside of the peptide binding groove and does not contact the TPI_{23-37} peptide. A comparison of the $HA_{306-318}$ peptide/HLA-DR1/SEC3-3B2 complex solved in a manner analogous to the structures presented here (E.J.S., P.S.A. & R.A.M., unpublished data) and the $HA_{306-318}$ peptide/HLA-DR1 structure solved in the absence of superantigen,[22] revealed that no significant structural changes exist in the MHC peptide binding groove or the $HA_{306-318}$ peptide on account of SEC3-3B2 binding (data not shown). Thus, it is likely that the presence of SEC3-3B2 in the wild-type and mutant TPI_{23-37} peptide/HLA-DR1/SEC3-3B2 complex structures does not affect the structure of the TPI_{23-37} peptides and how they are bound in the peptide binding groove of HLA-DR1.

Structural differences are confined to the mutation site

The wild-type and mutant TPI_{23-37} peptide/HLA-DR1/SEC3-3B2 complex structures exhibit very little structural deviation from one another, as shown in Figure 1(c). The TPI_{23-37} peptides from these structures are also highly superimposable (Figure 2(a)), and are bound in the HLA-DR1 peptide binding groove analogously (Figure 2(b)). These results confirm the binding register of the TPI_{23-37} peptides in the HLA-DR1 binding groove predicted previously with the mutation site residue at position P3.[17] The root mean square deviations for all atoms in the peptide chains is 0.44 Å, while for C^α atoms it is 0.19 Å. Most of the differences between the peptide structures are confined to their extreme N and C-terminal residues, Gly23 at position P3 and Asp37 at position P12, respectively, both of which extend beyond the ends of the HLA-DR1 peptide binding groove (Figure 2(b)). Furthermore, these residues are located outside of the TCR binding interface of a peptide/HLA-DR1 complex,[23] and thus, are unlikely to influence T cell stimulation *via* interaction with TCR molecules on the surface of $CD4^+$ TIL 1558, although functional assays have shown that peptide flanking residues that lie outside of the MHC anchor residues can influence T cell recognition.[24] Structural differences in the wild-type and mutant TPI_{23-37} peptide/HLA-DR1 complexes that most likely contribute to TCR interactions are therefore confined to the mutation site, a Thr residue in the wild-type peptide, but an Ile in the mutant peptide.

Extensive HLA-DR1 interactions of the mutation site residues

The side-chains of the mutation site residues in the TPI_{23-37} peptides diverge in structure only beyond their C^β atoms, located 0.17 Å apart, while the positions of their $C^{\gamma 2}$ atoms differ by a rotation about the C^α–C^β axis of 74° (Figure 3(a)). Although the mutation site at position P3 is not an MHC class II anchor residue, the conformations of their respective side-chains in the wild-type and mutant TPI_{23-37} peptides are such that they both make extensive interactions with the HLA-DR1 α subunit. Figure 3(b) shows these contacts made by Thr28 of the wild-type TPI_{23-37} peptide, including van der Waals interactions with residues Gln9, Phe22 and Phe54, as well as a hydrogen bonding network *via* two bridging water molecules to Asn55. Ile28 of mutant TPI_{23-37} likewise makes extensive contacts, including van der Waals interactions with Gln9, Phe22, Phe54, Gly58 and Asn62 (Figure 3(c)).

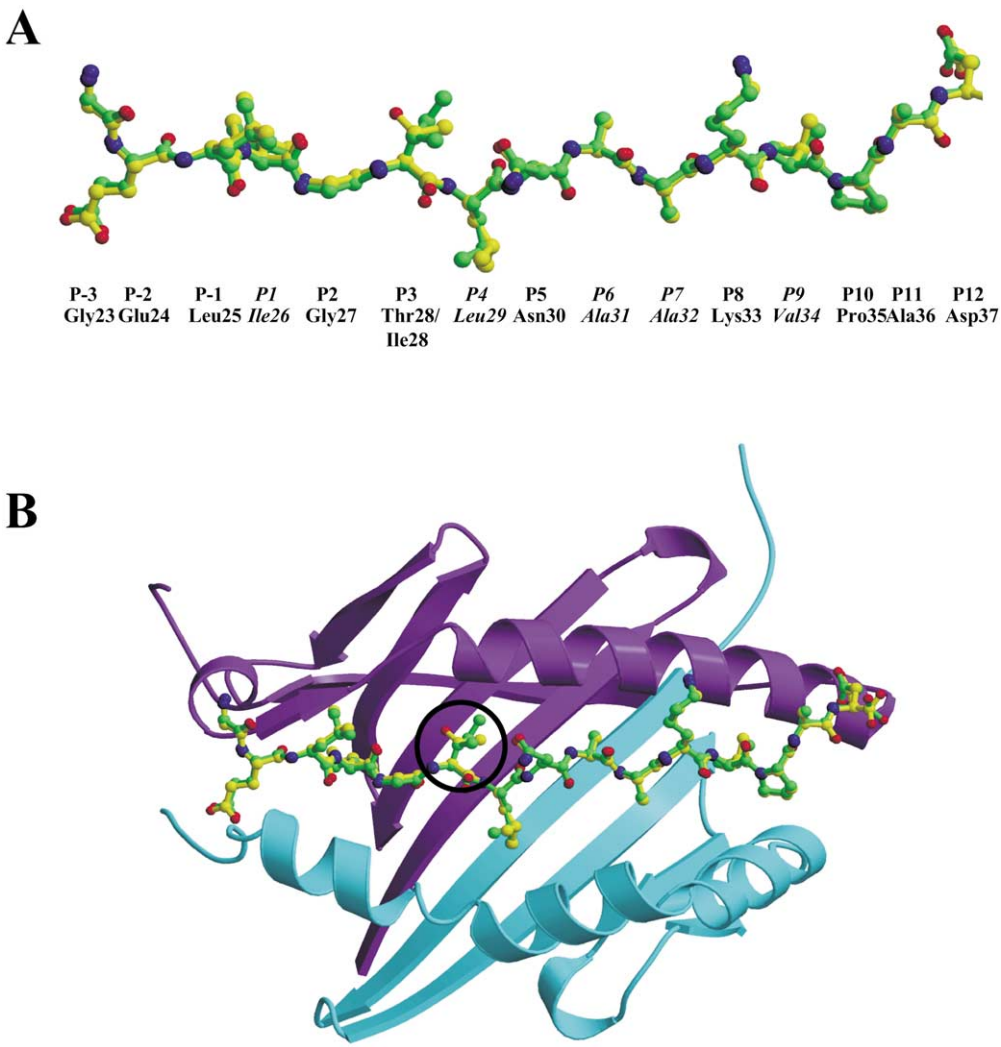

Figure 2. Conformations of the wild-type and mutant TPI_{23-37} peptides and their positions in the peptide binding groove of HLA-DR1 are nearly identical. (a) Superposition of wild-type (yellow) and mutant (green) TPI_{23-37} peptides as viewed from the top. Residue labels are aligned with the C^{α} atom of the respective residue. Pocket residues are labeled in italics, the mutation site is labeled in bold. (b) Top view of the wild-type and mutant TPI_{23-37} peptides bound in the peptide binding groove of HLA-DR1. The mutation site residue is circled. In all panels colors are as follows: wild-type TPI_{23-37} peptide, yellow; mutant TPI_{23-37} peptide, green; HLA-DR1 α chain, purple; HLA-DR1 β chain, cyan; nitrogen atoms, blue; oxygen atoms, red.

Analysis of the accessible surface area (ASA) of the mutation site residue 28 reveals the relative inaccessibility of much of both the wild-type Thr28 and mutant Ile28 side-chains (Table 2). Nearly all of the surface accessibilty in Thr28 derives from the nitrogen and oxygen atoms of the peptide main chain as well as the C^{β} atom. The remainder of the atoms in Thr28, including the main chain carbon atoms and the $O^{\gamma 1}$ and $C^{\gamma 2}$ atoms, are buried against the HLA-DR1 α chain, providing only 3 $Å^2$ of exposed surface. The surface accessibilty of Ile28 in the mutant TPI_{23-37} peptide is similar to that of the wild-type Thr28, with the polar main chain atoms and C^{β} exposed and the main chain carbon and the $C^{\gamma 1}$ and $C^{\delta 1}$ atoms inaccessible. The main differences in ASA between Thr28 and Ile28 are a result of the positional differences of the their $C^{\gamma 2}$ atoms.

Minor structural differences in antigenic surface presented to T cells

As the majority of both Thr28 of the wild-type peptide and Ile28 of the mutant peptide are packed against the HLA-DR1 α chain, there is little difference in molecular structure as would be encountered by a TCR molecule binding these two peptide–MHC (pMHC) class II complex surfaces. The only significant structural difference between the wild-type and mutant TPI_{23-37} peptide/HLA-DR1 complexes is due to the $C^{\gamma 2}$ atom of Ile28 in the mutant TPI_{23-37} peptide, which points towards the TCR molecule in a putative mutant TPI_{23-37} peptide/HLA-DR1/TCR complex, on account of the rotation of the mutant Ile28 side-chain about the C^{α}–C^{β} axis, relative to that of the wild-type Thr28 (Figure 3(a)).

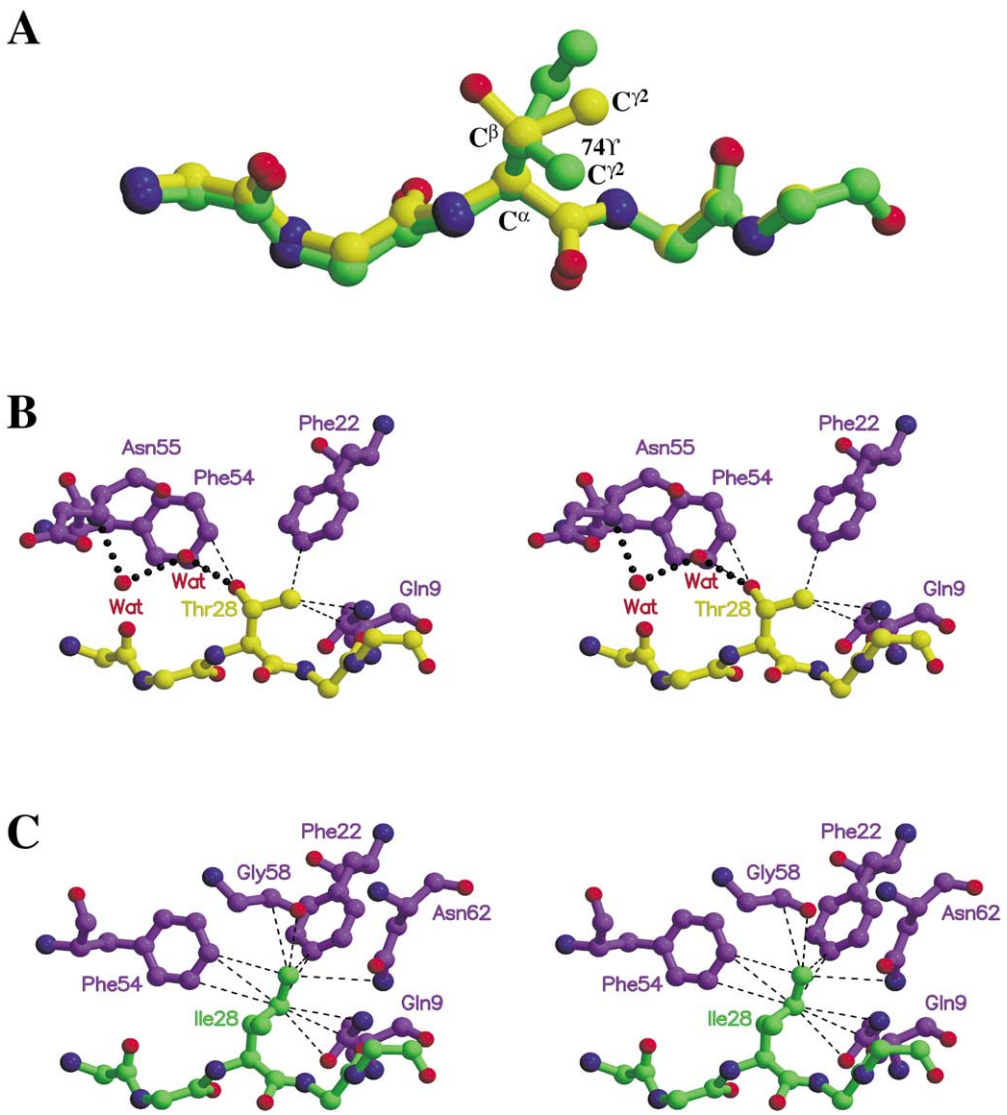

Figure 3. Both wild-type and mutant residues at position 28 of TPI_{23-37} make extensive contacts with the HLA-DR1 α chain. (a) Superposition of the wild-type (yellow) and mutant (green) TPI_{23-37} peptides, showing the mutation site residue. Stereo diagrams of intermolecular contacts formed between residues from the HLA-DR1 α chain and the side-chains of (b) residue Thr28 of the wild-type TPI_{23-37} peptide and (c) residue Ile28 of the mutant TPI_{23-37} peptide. Hydrogen bonds are depicted as dotted lines, van der Waals interactions by broken lines. Maximum contact distances (in Å) are as follows: C–C, 4.1; C–N, 3.8; C–O, 3.7; O–O, 3.3; O–N, 3.4; N–N, 3.4. In all panels, colors are as follows: wild-type TPI_{23-37} peptide, yellow; mutant TPI_{23-37} peptide, green; HLA-DR1 α chain, purple; HLA-DR1 β chain, cyan; nitrogen atoms, blue; oxygen atoms and water molecules, red. Side-chains of TPI_{23-37} peptide residues other than at the mutation site have been removed for clarity.

Accordingly, the molecular surfaces presented to T cells of HLA-DR1 complexed with both wild-type and mutant TPI_{23-37} peptides are highly similar. As shown in Figure 4, differences in the TPI_{23-37} peptide molecular surfaces are essentially restricted to the mutation site, outlined in black. These differences, however, are not so substantial. Analysis of the ASA at residue 28 (Table 2) shows that the total ASA for the mutant Ile28 is only 6 $Å^2$ greater than for the wild-type Thr28. The most significant difference in ASA between the two peptides is in apolar ASA, a difference of 12 $Å^2$, due primarily to relative rotations of these two side-chains (Figure 3(a)) that results in greater surface exposure of the $C^{\gamma 2}$ atom in Ile28 *versus* this same atom in Thr28. No significant differences in HLA-DR1 structure between the two complexes were observed (Figure 2(a)).

Both wild-type and mutant TPI_{23-37} peptides bind HLA-DR1 with high affinity

In light of the small structural differences in the wild-type and mutant TPI_{23-37} peptide/HLA-DR1 complexes and because peptide immunogenicity is known to be affected by pMHC complex stability,[25–27] we wished to know if HLA-DR1 bound the wild-type and mutant TPI_{23-37} peptides

Table 2. Accessible surface areas of the mutation site residue 28 in the wild-type and mutant TPI_{23-37} peptides

	Accessible surface area (Å^2)[a]	
	Wild-type Thr28	Mutant Ile28
Atom		
N	6	9
C^{α}	0	0
C^{β}	9	3
$O^{\gamma 1}$	2	na
$C^{\gamma 2}$	1	19
$C^{\gamma 1}$	na[b]	0
$C^{\delta 1}$	na	0
C	0	0
O	24	17
Total	42	48
Polar	32	26
Apolar	10	22

[a] Accessible surface areas calculated using the program AREAIMOL[65] and a sphere radius of 1.4 Å.
[b] Not applicable. Residue does not contain this atom.

with significantly different affinities that might contribute to the discrepancies in T cell stimulation capacities of these two peptides. Competition binding assays, however, revealed no appreciable difference in the 50% inhibitory concentration (IC_{50}) values for these peptides (Table 3), and by analogy their relative affinities for HLA-DR1. This is not surprising as none of the differences in sequence and structure for these peptides correspond to residues that occupy defined pockets in the HLA-DR1 binding groove. The only amino acid difference occurs at position P3, which is not bound in a defined pocket of the HLA-DR1 binding groove and thus is more likely to have an effect on T cell stimulation through interaction with TCR molecules than on pMHC stability. Both wild-type and mutant TPI_{23-37} peptides, in fact, are bound with high affinity by HLA-DR1, exhibiting IC_{50} values of 25 and 13 nM, respectively (Table 3).

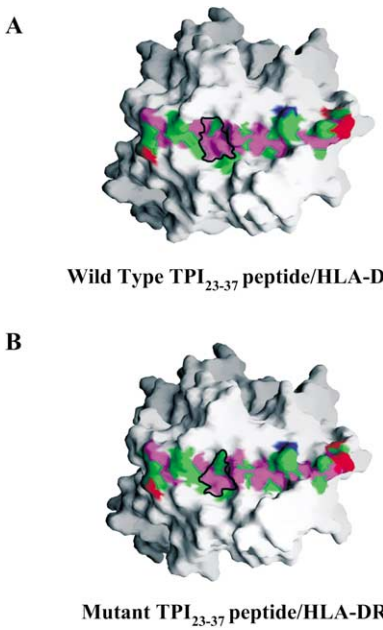

Figure 4. Very similar molecular surfaces are presented to the T cell receptor by HLA-DR1 complexed with both the wild-type and mutant TPI_{23-37} peptides. Molecular surface of HLA-DR1 complexed with (a) the wild-type TPI_{23-37} peptide and (b) the mutant TPI_{23-37} peptide. Color coding is as follows: green, carbon atoms; magenta, uncharged polar atoms; red, electronegative atoms; blue, electropositive atoms. The mutation site is outlined in black. Figure produced using GRASP.[64]

Table 3. HLA-DR1 binding characteristics of TPI_{23-37} and $HA_{306-318}$ peptides

Peptide	IC_{50} (nM)[a]	S_c[b]	S_c (solvated)[c]
Wild-type TPI_{23-37}	25	0.77	0.79
Mutant TPI_{23-37}	13	0.72	0.76
$HA_{306-318}$	5	0.79	0.80

[a] 50% Inhibitory concentation.
[b] Shape correlation value[28] as computed for peptide/HLA-DR1 interface. S_c is a measure of geometric match between two juxtaposed surfaces. Interfaces with perfect fits have an S_c value of 1, while interfaces that are topographically uncorrelated have S_c values of 0.
[c] S_c as computed for peptide plus bridging and buried solvent molecules/HLA-DR1.

Comparison of the mutant TPI_{23-37} peptide to others bound by HLA-DR1

The HLA-DR1 binding affinities of the TPI_{23-37} peptides are similar to that of another antigenic peptide corresponding to residues 306–318 of influenza hemaglutinin ($HA_{306-318}$; Table 3), which has an IC_{50} value of 5 nM, indicating a slightly more stable peptide–MHC complex. Shape complimentarity (S_c) values[28] calculated for the interfaces formed by the TPI_{23-37} and $HA_{306-318}$ peptides with HLA-DR1, with and without bridging and buried solvent molecules, however, are not significantly different (Table 3). In fact, the S_c values for all of these interfaces are as high or higher than those calculated for other high affinity complexes such as oligomeric proteins or protease–protease inhibitor complexes.[29]

A comparison of the $HA_{306-318}$ peptide/HLA-DR1/SEC3-3B2 (E.J.S., P.S.A. & R.A.M., unpublished data) and mutant TPI_{23-37} peptide/HLA-DR1/SEC3-3B2 crystal structures shows that the main chain conformation of these peptides bound in the HLA-DR1 binding groove are very similar, particularly in the region spanning the anchor residues P1, P4, P6, P7 and P9 (Figure 5(a)). Residues N-terminal and C-terminal to these core MHC class II binding residues diverge more in sequence, but not as significantly as when compared to peptides bound by other HLA-DR alleles.[30,31]

Southwood *et al*. (1998) have analyzed the HLA-DR binding capabilities of 384 synthetic peptides derived from naturally occurring sequences and

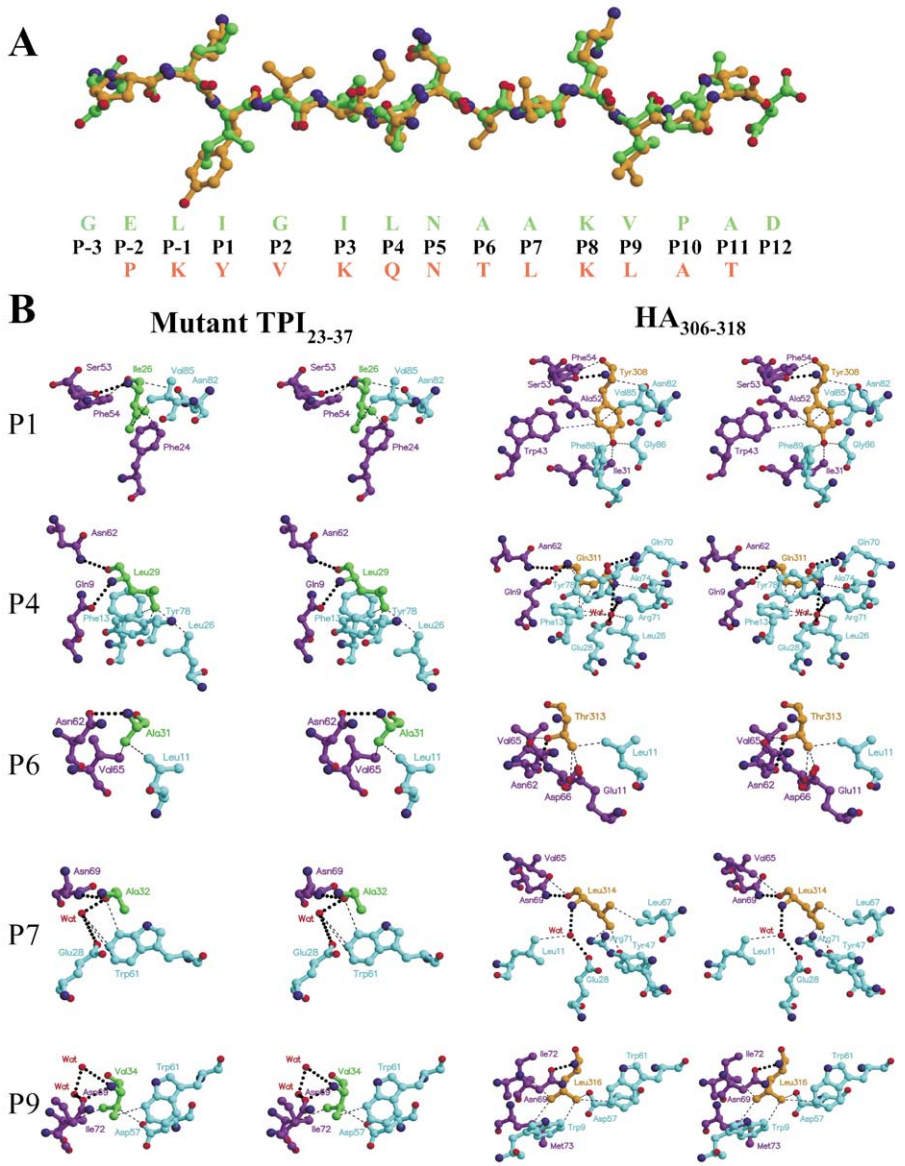

Figure 5. TPI_{23-37} and $HA_{306-318}$ peptides bind HLA-DR1 with high affinity utilizing distinct pocket residue interactions. (a) Superposition of the mutant TPI_{23-37} (green) and $HA_{306-318}$ (orange) peptides, as viewed from from the side, through the HLA-DR1 β chain (above) and peptide sequence alignment of the mutant TPI_{23-37} (green) and $HA_{306-318}$ (orange) peptides (below). Peptide sequence is aligned corresponding to the C^{α} atom of each residue. (b) Stereo diagrams of the HLA-DR1 P1, P4, P6, P7 and P9 pocket interactions for the mutant TPI_{23-27} (left) and $HA_{306-318}$ peptides (right). Hydrogen bonds are depicted as dotted lines, van der Waals interactions by broken lines. Maximum contact distances (in Å) are as follows: C–C, 4.1; C–N, 3.8; C–O, 3.7; O–O, 3.3; O–N, 3.4; N–N, 3.4. In all panels, colors are as follows: mutant TPI_{23-37} peptide, green; $HA_{306-318}$ peptide, orange; HLA-DR1 α chain, purple; HLA-DR1 β chain, cyan; nitrogen atoms, blue; oxygen atoms, red.

have calculated average relative binding (ARB) values for all 20 amino acids at each peptide residue position. This study has shown that nearly all peptides that bind with intermediate ($IC_{50} = 100–1000$ nM) or high ($IC_{50} \leq 100$ nM) affinity to HLA-DR1 require an aromatic or large hydrophobic residue at the P1 position (including Phe, Trp, Tyr, Leu, Ile, Val or Met) and a short and/or hydrophobic residue at the P6 position (including Ser, Thr, Cys, Ala, Pro, Val, Ile, Leu or Met). Also, secondary effects on peptide binding by HLA-DR1 were predominantly restricted to the other pocket residues at positions P4, P7 and P9, with the amino acid at P4 the most crucial of these.

While none of the pocket residues between the TPI_{23-37} and $HA_{306-318}$ peptides are the same (Figure 5(a)), both the TPI_{23-37} and $HA_{306-318}$ peptides satisfy the sequence requirements at P1 and P6 for high affinity HLA-DR1 binding. Additionally, TPI_{23-37} and $HA_{306-318}$ residues at the other pocket positions all correspond to amino acids with better than average ARB values.[32]

Figure 5(b) shows the intermolecular contacts made by each pocket residue in the mutant TPI_{23-37} (left column) and $HA_{306-318}$ peptides (right column) with HLA-DR1 residues and buried water molecules. Analogous interactions for the wild-type TPI_{23-37} peptide are not shown as they do not differ significantly from those made by the mutant peptide. The P1 position side-chains of the TPI_{23-37} and $HA_{306-318}$ peptide residues, the hydrophobic Ile26 and the aromatic Tyr308, respectively, each make multiple van der Waals interactions with both HLA-DR1 α and β chain residues to adequately fill this deep and apolar pocket. TPI_{23-37} Ala31 and $HA_{306-318}$ Thr313 are both short and hydrophobic enough to fit appropriately in the shallow P6 pocket. Our binding data reveal that the $HA_{306-318}$ peptide binds HLA-DR1 with a slightly higher affinity than do the TPI_{23-37} peptides (Table 3). This may be due to the relative interactions of the P4 position residues in these peptides. The side-chain of Leu29 of TPI_{23-37} makes three van der Waals interactions with residues from the HLA-DR1 α chain. The $HA_{306-318}$ Thr313 side-chain forms a similar set of van der Waals interactions, but additionally makes a direct hydrogen bond with one HLA-DR1 α chain residue and indirect hydrogen bonds to two other HLA-DR1 α chain residues *via* a bridging water molecule. Comparing ARB values for the P1, P4, P6, P7 and P9 pocket residues from the TPI_{23-37} and $HA_{306-318}$ peptides shows that these values differ by more than twofold only for the residues at position P4.[32] The TPI_{23-37} and $HA_{306-318}$ peptide residues at positions P7 and P9 form similar contacts with HLA-DR1 and likely do not affect the relative stabilities of the complexes significantly.

One additional structure of a single peptide bound to HLA-DR1 exists in the Protein Data Bank, the complex formed with an endogenous peptide derived from residues 103–117 of the MHC class I molecule HLA-A2 ($A2_{103-117}$).[33] The $A2_{103-117}$ peptide constitutes the predominant naturally processed peptide bound to HLA-DR1,[34] in part due to its relatively high stability ($IC_{50} = 49$ nM). The $A2_{103-117}$ peptide adopts the extended polyproline II-like conformation within the HLA-DR1 peptide binding groove common to the TPI_{23-37} and $HA_{306-318}$ peptides and satisfies the sequence requirements of high affinity HLA-DR1 binding peptides with a Trp residue at position P1 and a Gly residue at position P6. In the secondary pocket positions, the $A2_{103-117}$ peptide has the following residues: Leu (P4); Tyr (P7); and Gln (P9). The P4 residue of the $A2_{103-117}$ peptide is the same as that found in the TPI_{23-37} peptides. The ARB value of the Tyr residue at position P7 is not significantly different from those for the P7 residues of the TPI_{23-37} and $HA_{306-318}$ peptides.[32] The lower affinity of the $A2_{103-117}$ peptide may derive primarily from its P9 residue, whose ARB value is more than twofold lower than for those residues at the P9 position in either the TPI_{23-37} and $HA_{306-318}$ peptides.[32]

Discussion

The immunogenicity of antigens depends on a number of factors, including the intracellular processing of proteins into peptidic fragments, their loading into MHC molecules and subsequent presentation on the cell surface, the stability of the pMHC complex and the structure of the pMHC complex molecular surface in the TCR interface region. Only the last of these factors likely plays a role in the T cell stimulation discrepancy observed between the wild-type and mutant TPI_{23-37} peptides. While it is possible, although unlikely, that the processing and MHC loading characteristics of wild-type and mutant TPI_{23-37} differ substantially enough to affect T cell stimulation *in vivo*, the differences in T cell stimulation for the TPI_{23-37} peptides were observed *in vitro* using synthetic peptides pulsed onto the surfaces of APCs.[17] Likewise, differential pMHC stability of the wild-type and mutant TPI peptides cannot explain the stimulation discrepancy as measurements presented here revealed no appreciable relative difference in the stabilities of these pMHC complexes.

Instead, the seemingly inconsequential structural differences observed in the wild-type and mutant TPI_{23-37} peptide/HLA-DR1 structures most likely cause the dramatic enhancement of T cell stimulation by the mutant TPI_{23-37} antigen. In the absence of structural data, the position of the mutation site residue and the relative chemical natures of the wild-type Thr and mutant Ile side-chains both would seem to belie their impact on T cell activation. The mutation site residue does indeed occupy a peptide register position that allows for potential productive interactions with TCR molecules, as seen in two pMHC class II/TCR crystal structures.[23,35] The TPI_{23-37} peptide/HLA-DR1 crystal structures presented here, however, reveal that the majority of both wild-type and mutant side-chains are largely inaccessible to any interacting surface. The side-chain conformations of both wild-type and mutant residues, due to rotation about the C^{β} atom, result in burial of most side-chain atoms against the HLA-DR1 α subunit side of the peptide binding groove. This effectively removes differences in the chemical nature of the Thr and Ile side-chains, especially differences in polarity, as an important distinction for TCR engagement. The only atom from these two residues that has significant surface accessibility is the Ile $C^{\gamma 2}$ atom. Thus, it seems that the structural basis for disparities in T cell stimulation caused by the wild-type and mutant TPI_{23-37} peptides is primarily dependent on the surface exposure of a single methyl group.

Because all knowledge of the T cell stimulation differences between the wild-type and mutant

TPI_{23-37} peptide antigens derives from studies using TIL 1558,[17] an oligoclonal cell line, the sequence of the particular TCR molecule that interacts specifically with TPI_{23-37} peptide/HLA-DR1 is unknown currently, although efforts to identify this TCR are underway. In the absence of such data, only hypotheses concerning the characteristics of the potential TCR contacts responsible for the dramatic stimulation differences between the wild-type and mutant TPI_{23-37} peptide antigens based on the structural results reported here can be made.

The complex of the $HA_{306-318}$ peptide/HLA-DR1/HA1.7 αβTCR[23] exists as the sole example of a pMHC/TCR structure involving HLA-DR1. In this complex, the $HA_{306-318}$ peptide residue at position P3, Lys310, forms a salt bridge with Glu102 of the TCR α chain complimentarity determining region (CDR) 3 loop and van der Waals contacts with CDR3β Thr97, both *via* its N^{ζ} atom. The CDR3 loops of the HA1.7 αβTCR are relatively long (14 residues for both TCR α and β chains), facilitating these interactions. No intermolecular contacts are formed between Lys310 and the CDR1 or CDR2 loops of the HA1.7 TCR α or β chains. The corresponding wild-type and mutant TPI_{23-37} peptide residues at the mutation site position P3, Thr28 and Ile28, possess significantly shorter side-chains than does Lys310 of the $HA_{306-318}$ peptide. It follows that in order to make productive interactions with TPI_{23-37} residue 28, the functional TCR of TIL 1558 is likely to possess CDR3 loops of at least equivalent length to those in the HA1.7 αβTCR and to be found in a highly extended conformation. As the exposed molecular surfaces of residue 28 in the wild-type and mutant TPI_{23-37} peptides are apolar, it is most probable that any TCR residues that directly contact this residue in this pMHC/TCR complex will also be of a hydrophobic nature so as to maximize the differential effect on complex formation.

The structural differences between the wild-type and mutant TPI_{23-37} peptide/HLA-DR1 complexes can be expressed in terms of ASA changes in the molecular surface caused by the single amino acid mutation. For the reasons stated above, the TPI_{23-37} peptide/HLA-DR1 molecular surface difference most likely to affect TCR binding is the 12 $Å^2$ relative increase in apolar ASA for the mutant *versus* wild-type complex (Table 2). Previously, we established a correlation between binding free energy and apolar ASA in a protein–protein interface corresponding to 21 cal mol^{-1} $Å^{-2}$.[36] This estimate of the hydrophobic effect predicts a difference in binding free energy between the putative wild-type and mutant pMHC/TCR complexes of 0.25 kcal mol^{-1}, assuming that the entire difference in apolar ASA is buried by the interacting TCR molecule. This corresponds to a change in affinity in the putative pMHC/TCR complexes of 0.5-fold starting from an initial affinity of 1 μM, which is within the affinity range for known stimulatory pMHC–TCR complexes.[37]

Differential affinities of the putative wild-type and mutant pMHC/TCR complexes could also result from the formation of cavities within the protein interface around residue 28. The free energy cost of cavity formation in the protein core has been estimated[38] and may be extendable to the energetics at a protein–protein interface. This presents the possibility that complex formation between the TIL 1558 functional TCR and the wild-type and mutant TPI_{23-37} peptide/HLA-DR1 complexes could be regulated, in whole or in part, by relative interface cavity size. This assumes that a larger cavity is formed within the interface involving the wild-type TPI_{23-37} peptide, relative to the mutant, resulting in a lower affinity pMHC/TCR complex. It remains possible then that the TIL 1558 functional TCR makes no contacts with the mutation site residue 28 of the wild-type or mutant TPI_{23-37} peptides, but that this amino acid change is still responsible for altered pMHC/TCR complex affinity and T cell stimulation.

Any changes in affinity due to the differences in buried apolar ASA or relative cavity size will appear insignificant when compared to the five log-fold enhancement in T cell stimulation caused by the mutation of TPI_{23-37} residue 28 from Thr to Ile. Significant effects on T cell activation as a result of small structural differences in pMHC complex surface, though, appear to be more the norm than the exception, as shown for a number of pMHC class I/TCR systems through structural and cellular studies.[39–42] In one of these studies[40] N-alkylated amino acid substitution at a peptide position that is not contacted by TCR was implemented to repair stepwise, through the addition of methyl groups, a defect in the pMHC/TCR interface. This defect originated from a Pro to Ala mutation, the effective removal of two methyl groups, which converted the peptide antigen from an agonist to an antagonist, concomitant with several orders of magnitude reduction in T cell activation.[39] Reintroduction of one of the missing methyl groups, *via* an *N*-ethyl glycine substitution, resulted in a strong agonist peptide with similar pMHC/TCR complex interaction kinetics to that of a peptide bearing the wild-type Pro residue and exhibited fully restored T cell stimulatory capacity. The wild-type and mutant TPI_{23-37}/HLA-DR1 crystal structures suggest that MHC class II-restricted tumor antigens may follow a similar principle, where structural differences as small as a single methyl group exposed to TCR can result in dramatically altered T cell stimulation.

How then can such small structural differences correspond to such dramatic enhancements of T cell activation? While it is unknown at present, a number of possibilities exist. (1) It may be that the Thr to Ile mutation in TPI_{23-37} results in a pMHC/TCR complex with a half-life above a threshold required for effective T cell stimulation. Even though a number of studies[39,41,43–45] have revealed some reasonable correlation between pMHC/TCR complex half-lives and T cell stimulation,

others[40,43,46–48] have shown that for some systems this correlation does not hold. (2) The possible existence of preformed TCR dimers on the T cell surface[49] suggests that T cell stimulation may be affected to some extent by TCR dimer conformational changes (i.e. reorientation of TCR monomers relative to one another) upon interaction with pMHC complexes. The resultant cooperative or allosteric characteristics of the pMHC/TCR interaction could impart greater significance to small structural changes, such as those between the wild-type and mutant TPI_{23-37}/HLA-DR1 complexes, than would otherwise be expected in a 1:1 interaction. (3) Formation of pMHC/TCR complexes occurs at the cell–cell interface where they are subjected to mechanical stress.[50] The mechanical strength of a non-covalent bond is highly correlated to the activation enthalpy of the interaction, for which extremely high values have been measured in several pMHC/TCR interactions.[51,52] It may be that the structural differences between the wild-type and mutant TPI_{23-37}/HLA-DR1 complexes have a large impact on their respective activation enthalpies upon interaction with TCR.

The TPI_{23-37}/HLA-DR1 complex structures presented here comprise the first structural analysis of tumor antigens capable of stimulating $CD4^+$ T cells. Our results show that MHC class II-restricted tumor antigens are likely to follow the general rules for T cell stimulation by other peptide antigens and reveal that seemingly inconsequential structural changes can have unexpectedly dramatic effects on T cell activation. Defining the structural basis for T cell stimulation by MHC class II-restricted tumor antigens is an important step in the design of immunotherapy reagents that will specifically activate the critical anti-tumor response of $CD4^+$ HTLs.

Materials and Methods

Recombinant protein expression and purification for crystallographic analysis

HLA-DR1 was produced by *in vitro* refolding from *Escherichia coli* inclusion bodies in the presence of either wild-type or mutant TPI_{23-37} peptide (Research Genetics) and purified according to published methods.[53] SEC3-3B2 was expressed as a soluble protein in *E. coli* and isolated from the periplasmic fraction as described.[19]

Crystallization and data collection

Crystals of the wild-type and mutant TPI_{23-37} peptides in complex with HLA-DR1 and SEC3-3B2 were grown at room temperature by hanging drop vapor diffusion by mixing 1 μl of complex solution (containing an equimolar ratio of TPI_{23-37} peptide/HLA-DR1 complex and SEC3-3B2 at a total concentration of 10 mg/ml) with an equal volume of reservoir solution containing 0.1 M sodium acetate (pH 5.2), 10% (w/v) ethylene glycol and 2–4% (w/v) polyethylene glycol 4000. Crystals were transferred to cryoprotectant solution (mother liquor containing 25% ethylene glycol) just prior to mounting and flash-cooling in the liquid nitrogen stream. X-ray diffraction data were collected on a Brandeis B4 CCD detector from single crystals at 100 K at beamline X-12C of the National Synchrotron Light Source, Brookhaven National Laboratory. The wild-type and mutant TPI_{23-37} peptide/HLA-DR1/SEC3-3B2 complexes crystallized isomorphously. Diffraction data were treated independently for both crystals and were processed and scaled using DENZO and SCALEPACK.[54] Data collection statistics are shown in Table 1.

Structure determination and refinement

The structures of the wild-type and mutant TPI_{23-37} peptide/HLA-DR1/SEC3-3B2 complexes were solved independently by molecular replacement methods using the program AMoRe,[55] with crystal structures of HLA-DR1 (PDB accession code 1SEB) and wild-type SEC3[21] as search models. The solution for HLA-DR1 was found first and its position fixed in order to locate SEC3. The initial model solutions gave correlation coefficients of 48.2% and 51.9% and R_{factor} values of 52.8% and 52.3% at a resolution range of 15–3.5 Å for the wild-type and mutant structures, respectively. Refinement was carried out using CNS,[56] including rigid-body refinement, iterative cycles of positional, torsion angle and temperature factor (B) refinement, interspersed with model rebuilding into σ_A-weighted $F_o - F_c$ and $2F_o - F_c$ electron density maps using XtalView.[57] Water molecules were added only to $F_o - F_c$ density higher than 3σ and standard hydrogen-bonding geometry. The wild-type and mutant structures were refined to R_{cryst} values of 20.8% and 20.5% and R_{free} values of 22.0% and 24.5%, respectively. Current refinement statistics for the complex structures are summarized in Table 1. Due to poor or non-existent electron density, the final wild-type structure model is missing residues 1–3 of the HLA-DR1 α chain and 97–105 of SEC3-3B2, while the final mutant structure model is missing residues 1–3 and 181–182 of the HLA-DR1 α chain, 108–110 of the HLA-DR1 β chain and 99–106 of SEC3-3B2.

HLA-DR1 peptide-binding assays

The HLA-DR1 peptide-binding assays for the TPI_{23-37} and $HA_{306-318}$ peptides were performed as described.[32] Briefly, HLA-DR1 molecules were purified from LG2 cells by affinity chromatography according to published methods[58,59] using the monoclonal antibody LB3.1 coupled to Sepharose CL4B beads. Purified HLA-DR1 (5–500 nM) was incubated with various unlabeled peptide inhibitors and 1–10 nM ^{125}I-radiolabeled probe peptides for 48 hours in PBS containing 5%(v/v) DMSO and 0.05%(v/v) Nonidet P-40 in the presence of protease inhibitors at pH 7.0. Peptide/HLA-DR1 complexes were separated from free peptide by gel filtration, and the fraction of bound peptide calculated as described.[58] In preliminary experiments, the HLA-DR1 preparation was titered in the presence of fixed amounts of radiolabeled peptides to determine the concentration necessary to bind 15–25% of the total radioactivity. All subsequent inhibition and direct binding assays were then performed using these concentrations. Radiolabeled $HA_{307-319}$ peptide was iodinated using the chloramine-T method.[60] Peptide inhibitors were tested at concentrations ranging from 12 μg/ml to 120 pg/ml, yielding the dose corresponding to 50% inhibitory concentration

(IC_{50}). In appropriate stoichiometric conditions, the IC_{50} of an unlabeled test peptide to the purified HLA-DR1 is a reasonable approximation of the affinity of interaction (K_d). Peptides were tested in two to four completely independent experiments.

Protein Data Bank accession codes

The coordinates and structure factors for the wild-type and mutant TPI_{23-37} peptide/HLA-DR1/SEC3-3B2 complexes have been deposited in the Protein Data Bank with accession codes 1KLU and 1KLG, respectively.

Acknowledgments

We thank the staff at beamline X-12C National Synchrotron Light Source, Brookhaven National Laboratory for assistance in data collection and Dr Suzanne L. Topalian (National Cancer Institute, National Institutes of Health (NIH)) for helpful discussions and critical reading of the manuscript. This research was supported by NIH grants AI36900 and AI49564 (R.A.M.). E.J.S. is supported by a fellowship from the Arthritis Foundation.

References

1. Rosenberg, S. A., Yang, J. C., Schwartzentruber, D. J., Hwu, P., Marincola, F. M., Topalian, S. L. *et al.* (1998). Immunologic and therapeutic evaluation of a synthetic peptide vaccine for the treatment of patients with metastatic melanoma. *Nature Med.* **4**, 321–327.
2. Nestle, F. O., Alijagic, S., Gilliet, M., Sun, Y., Grabbe, S., Dummer, R. *et al.* (1998). Vaccination of melanoma patients with peptide- or tumor lysate-pulsed dendritic cells. *Nature Med.* **4**, 328–332.
3. Marchand, M., van Baren, N., Weynants, P., Brichard, V., Dreno, B., Tessier, M. H. *et al.* (1999). Tumor regressions observed in patients with metastatic melanoma treated with an antigenic peptide encoded by gene MAGE-3 and presented by HLA-A1. *Int. J. Cancer*, **80**, 219–230.
4. Dallal, R. M. & Lotze, M. T. (2000). The dendritic cell and human cancer vaccines. *Curr. Opin. Immunol.* **12**, 583–588.
5. Toes, R. E., Ossendorp, F., Offringa, R. & Melief, C. J. (1999). CD4 T cells and their role in antitumor immune responses. *J. Exp. Med.* **189**, 753–756.
6. Cohen, P. A., Peng, L., Plautz, G. E., Kim, J. A., Weng, D. E. *et al.* (2000). CD4+ T cells in adoptive immunotherapy and the indirect mechanism of tumor rejection. *Crit. Rev. Immunol.* **20**, 17–56.
7. Wang, R. F. (2001). The role of MHC class II-restricted tumor antigens and CD4+ T cells in antitumor immunity. *Trends Immunol.* **22**, 269–276.
8. Zeng, G. (2001). MHC class II-restricted tumor antigens recognized by CD4 + T cells: new strategies for cancer vaccine design. *J. Immunother.* **24**, 195–204.
9. Ossendorp, F., Mengede, E., Camps, M., Filius, R. & Melief, C. J. (1998). Specific T helper cell requirement for optimal induction of cytotoxic T lymphocytes against major histocompatibility complex class II negative tumors. *J. Exp. Med.* **187**, 693–702.
10. Mackey, M. F., Gunn, J. R., Ting, P. P., Kikutani, H., Dranoff, G., Noelle, R. J. *et al.* (1997). Protective immunity induced by tumor vaccines requires interaction between CD40 and its ligand, CD154. *Cancer Res.* **57**, 2569–2574.
11. Mackey, M. F., Gunn, J. R., Maliszewsky, C., Kikutani, H., Noelle, R. J. & Barth, R. J., Jr (1998). Dendritic cells require maturation *via* CD40 to generate protective antitumor immunity. *J. Immunol.* **161**, 2094–2098.
12. Schoenberger, S. P., Toes, R. E., van der Voort, E. I., Offringa, R. & Melief, C. J. (1998). T-cell help for cytotoxic T lymphocytes is mediated by CD40–CD40L interactions. *Nature*, **393**, 480–483.
13. Bennett, S. R., Carbone, F. R., Karamalis, F., Flavell, R. A., Miller, J. F. & Heath, W. R. (1998). Help for cytotoxic-T-cell responses is mediated by CD40 signalling. *Nature*, **393**, 478–480.
14. Ridge, J. P., Di Rosa, F. & Matzinger, P. (1998). A conditioned dendritic cell can be a temporal bridge between a CD4+ T-helper and a T-killer cell. *Nature*, **393**, 474–478.
15. Marzo, A. L., Kinnear, B. F., Lake, R. A., Frelinger, J. J., Collins, E. J., Robinson, B. W. *et al.* (2000). Tumor-specific CD4+ T cells have a major post-licensing role in CTL mediated anti-tumor immunity. *J. Immunol.* **165**, 6047–6055.
16. Wang, R. F., Wang, X., Atwood, A. C., Topalian, S. L. & Rosenberg, S. A. (1999). Cloning genes encoding MHC class II-restricted antigens: mutated CDC27 as a tumor antigen. *Science*, **284**, 1351–1354.
17. Pieper, R., Christian, R. E., Gonzales, M. I., Nishimura, M. I., Gupta, G., Settlage, R. E. *et al.* (1999). Biochemical identification of a mutated human melanoma antigen recognized by CD4+ T cells. *J. Exp. Med.* **189**, 757–766.
18. Dessen, A., Lawrence, C. M., Cupo, S., Zaller, D. M. & Wiley, D. C. (1997). X-ray crystal structure of HLA-DR4 (DRA*0101, DRB1*0401) complexed with a peptide from human collagen II. *Immunity*, **7**, 473–481.
19. Andersen, P. S., Lavoie, P. M., Sekaly, R. P., Churchill, H., Kranz, D. M., Schlievert, P. M. *et al.* (1999). Role of the T cell receptor α chain in stabilizing TCR–superantigen–MHC class II complexes. *Immunity*, **10**, 473–483.
20. Jardetzky, T. S., Brown, J. H., Gorga, J. C., Stern, L. J., Urban, R. G., Chi, Y. I. *et al.* (1994). Three-dimensional structure of a human major histocompatibility molecule complexed with superantigen. *Nature*, **368**, 711–718.
21. Deringer, J. R., Ely, R. J., Stauffacher, C. V. & Bohach, G. A. (1996). Subtype-specific interactions of type C staphylococcal enterotoxins with the T-cell receptor. *Mol. Microbiol.* **22**, 523–534.
22. Stern, L. J., Brown, J. H., Jardetzky, T. S., Gorga, J. C., Urban, R. G., Strominger, J. L. *et al.* (1994). Crystal structure of the human class II MHC protein HLA-DR1 complexed with an influenza virus peptide. *Nature*, **368**, 215–221.
23. Hennecke, J., Carfi, A. & Wiley, D. C. (2000). Structure of a covalently stabilized complex of a human αβ T cell receptor, infulenza HA peptide and MHC class II molecule, HLA-DR1. *EMBO J.* **19**, 5611–5624.
24. Carson, R. T., Vignali, K. M., Woodland, D. L. & Vignali, D. A. (1997). T cell receptor recognition of MHC class II-bound peptide flanking residues enhances immunogenicity and results in altered TCR V region usage. *Immunity*, **7**, 387–399.

25. Kirksey, T. J., Pogue-Caley, R. R., Frelinger, J. A. & Collins, E. J. (1999). The structural basis for the increased immunogenicity of two HIV-reverse transcriptase peptide variant/class I major histocompatibility complexes. *J. Biol. Chem.* **274**, 37259–37264.
26. Uger, R. A., Chan, S. M. & Barber, B. H. (1999). Covalent linkage to beta2-microglobulin enhances the MHC stability and antigenicity of suboptimal CTL epitopes. *J. Immunol.* **162**, 6024–6028.
27. Grohmann, U., Belladonna, M. L., Bianchi, R., Orabona, C., Silla, S., Squillacioti, G. *et al.* (1999). Immunogenicity of tumor peptides: importance of peptide length and stability of peptide/MHC class II complex. *Cancer Immunol. Immunother.* **48**, 195–203.
28. Lawrence, M. C. & Colman, P. M. (1993). Shape complementarity at protein/protein interfaces. *J. Mol. Biol.* **234**, 946–950.
29. Jones, S. & Thornton, J. M. (1996). Principles of protein–protein interactions. *Proc. Natl Acad. Sci. USA*, **93**, 13–20.
30. Smith, K. J., Pyrdol, J., Gauthier, L., Wiley, D. C. & Wucherpfennig, K. W. (1998). Crystal structure of HLA-DR2 (DRA*0101, DRB1*1501) complexed with a peptide from human myelin basic protein. *J. Exp. Med.* **188**, 1511–1520.
31. Li, Y., Li, H., Martin, R. & Mariuzza, R. A. (2000). Structural basis for the binding of an immunodominant peptide from myelin basic protein in different registers by two HLA-DR2 proteins. *J. Mol. Biol.* **304**, 177–188.
32. Southwood, S., Sidney, J., Kondo, A., del Guercio, M.-F., Appella, E., Hoffman, S. *et al.* (1998). Several common HLA-DR types share largely overlapping peptide binding repertoires. *J. Immunol.* **160**, 3363–3373.
33. Murthy, V. L. & Stern, L. J. (1997). The class II MHC protein HLA-DR1 in complex with an endogenous peptide: implications for the structural basis of the specificity of peptide binding. *Structure*, **5**, 1385–1396.
34. Chicz, R. M., Urban, R. G., Lane, W. S., Gorga, J. C., Stern, L. J., Vignali, D. A. & Strominger, J. L. (1992). Predominant naturally processed peptides bound to HLA-DR1 are derived from MHC-related molecules and are heterogeneous in size. *Nature*, **358**, 764–768.
35. Reinherz, E. L., Tan, K., Tang, L., Kern, P., Liu, J., Xiong, Y. *et al.* (1999). The crystal structure of a T cell receptor in complex with peptide and MHC class II. *Science*, **286**, 1913–1921.
36. Sundberg, E. J., Urrutia, M., Braden, B. C., Isern, J., Tsuchiya, D., Fields, B. A. *et al.* (2000). Estimation of the hydrophobic effect in an antigen–antibody protein–protein interface. *Biochemistry*, **39**, 15375–15387.
37. Davis, M. M., Boniface, J. J., Reich, Z., Lyons, D., Hampl, J., Arden, B. & Chien, Y. (1998). Ligand recognition by alpha beta T cell receptors. *Annu. Rev. Immunol.* **16**, 523–544.
38. Eriksson, A. E., Baase, W. A., Zhang, X. J., Heinz, D. W., Blaber, M., Baldwin, E. P. & Matthews, B. W. (1992). Response of a protein structure to cavity-creating mutations and its relation to the hydrophobic effect. *Science*, **255**, 178–183.
39. Ding, Y. H., Baker, B. M., Garboczi, D. N., Biddison, W. E. & Wiley, D. C. (1999). Four A6-TCR/peptide/HLA-A2 structures that generate very different T cell signals are nearly identical. *Immunity*, **11**, 45–56.
40. Baker, B. M., Gagnon, S. J., Biddison, W. E. & Wiley, D. C. (2000). Conversion of a T cell antagonist into an agonist by repairing a defect in the TCR/peptide/MHC interface: implications for TCR signaling. *Immunity*, **13**, 475–484.
41. Degano, M., Garcia, K. C., Apostolopoulos, V., Rudolph, M. G., Teyton, L. & Wilson, I. A. (2000). A functional hot spot for antigen recognition in a superagonist TCR/MHC complex. *Immunity*, **12**, 251–261.
42. Ostrov, D. A., Roden, M. M., Shi, W., Palmieri, E., Christianson, G. J., Mendoza, L. *et al.* (2002). How H13 histocompatibility peptides differing by a single methyl group and lacking conventional MHC binding anchor motifs determine self-nonself discrimination. *J. Immunol.* **168**, 283–289.
43. Alam, S. M., Travers, P. J., Wung, J. L., Nasholds, W., Redpath, S., Jameson, S. C. *et al.* (1996). T-cell-receptor affinity and thymocyte positive selection. *Nature*, **381**, 616–620.
44. Lyons, D. S., Lieberman, S. A., Hampl, J., Boniface, J. J., Chien, Y., Berg, L. J. *et al.* (1996). A TCR binds to antagonist ligands with lower affinities and faster dissociation rates than to agonists. *Immunity*, **5**, 53–61.
45. Kersh, G. J., Kersh, E. N., Fremont, D. H. & Allen, P. M. (1998). High- and low-potency ligands with similar affinities for the TCR: the importance of kinetics in TCR signaling. *Immunity*, **9**, 817–826.
46. al-Ramadi, B. K., Jelonek, M. T., Boyd, L. F., Margulies, D. H. & Bothwell, A. L. (1995). Lack of strict correlation of functional sensitization with the apparent affinity of MHC/peptide complexes for the TCR. *J. Immunol.* **155**, 662–673.
47. Sykulev, Y., Vugmeyster, Y., Brunmark, A., Ploegh, H. L. & Eisen, H. N. (1998). Peptide antagonism and T cell receptor interactions with peptide–MHC complexes. *Immunity*, **9**, 475–483.
48. Baker, B. M., Turner, R. V., Gagnon, S. J., Wiley, D. C. & Biddison, W. E. (2001). Identification of a crucial energetic footprint on the alpha1 helix of human histocompatibility leukocyte antigen (HLA)-A2 that provides functional interactions for recognition by tax peptide/HLA-A2-specific T cell receptors. *J. Exp. Med.* **193**, 551–562.
49. Fernandez-Miguel, G., Alarcon, B., Iglesias, A., Bluethmann, H., Alvarez-Mon, M., Sanz, E. *et al.* (1999). Multivalent structure of an alphabetaT cell receptor. *Proc. Natl Acad. Sci. USA*, **96**, 1547–1552.
50. van der Merwe, P. A. (2001). The TCR triggering puzzle. *Immunity*, **14**, 665–668.
51. Boniface, J. J., Reich, Z., Lyons, D. S. & Davis, M. M. (1999). Thermodynamics of T cell receptor binding to peptide–MHC: evidence for a general mechanism of molecular scanning. *Proc. Natl Acad. Sci. USA*, **96**, 11446–11451.
52. Willcox, B. E., Gao, G. F., Wyer, J. R., Ladbury, J. E., Bell, J. I., Jakobsen, B. K. *et al.* (1999). TCR binding to peptide–MHC stabilizes a flexible recognition interface. *Immunity*, **10**, 357–365.
53. Frayser, M., Sato, A. K., Xu, L. & Stern, L. J. (1999). Empty and peptide-loaded class II major histocompatibility complex proteins produced by expression in *Escherichia coli* and folding *in vitro*. *Protein. Expr. Purif.* **15**, 105–114.
54. Otwinowski, Z. & Minor, W. (1997). Processing X-ray diffraction data collected in oscillation mode. *Methods Enzymol.* **276**, 307–326.
55. Navaza, J. (1994). AMoRe: an automated package for molecular replacement. *Acta Crystallog. sect. D* **50**, 157–163.

56. Brünger, A. T., Adams, P. D., Clore, G. M., DeLano, W. L., Gros, P., Grosse-Kunstleve, R. W. *et al.* (1998). Crystallography and NMR system: a new software suite for macromolecular structure determination. *Acta Crystallog. sect. D* **54**, 905–921.
57. McRee, D. E. (1999). XtalView/Xfit—a versatile program for manipulating atomic coordinates and electron density. *J. Struct. Biol.* **125**, 156–165.
58. Sette, A., Buus, S., Colon, S., Miles, C. & Grey, H. M. (1989). Structural analysis of peptides capable of binding to more than one Ia antigen. *J. Immunol.* **142**, 35–40.
59. Gorga, J. C., Horejsi, V., Johnson, D. R., Raghupathy, R. & Strominger, J. L. (1987). Purification and characterization of class II histocompatibility antigens from a homozygous human B cell line. *J. Biol. Chem.* **262**, 16087–16094.
60. Buus, S., Sette, A., Colon, S. M., Miles, C. & Grey, H. M. (1987). The relation between major histocompatibility complex (MHC) restriction and the capacity of Ia to bind immunogenic peptides. *Science*, **235**, 1353–1358.
61. Esnouf, R. M. (1997). An extensively modified version of MOLSCRIPT that includes greatly enhanced coloring capabilities. *J. Mol. Graph.* **15**, 132–134.
62. Merritt, E. A. & Bacon, D. J. (1997). Raster3D: photorealistic molecular graphics. *Methods Enzymol.* **277**, 505–524.
63. Kraulis, P. J. (1991). MOLSCRIPT: a program to produce both detailed and schematic plots of protein structures. *J. Appl. Crystallog.* **24**, 946–950.
64. Nicholls, A., Sharp, K. A. & Honig, B. (1991). Protein folding and association: insights from the interfacial and thermodynamic properties of hydrocarbons. *Proteins: Struct. Funct. Genet.* **11**, 281–296.
65. Collaborative Computational Project, Number 4 (1994). The CCP4 suite: programs for protein crystallography. *Acta Crystallog. sect. D*, **50**, 760–763.

Edited by I. Wilson

(Received 29 January 2002; received in revised form 9 April 2002; accepted 11 April 2002)